# Microstructure and Spectroscopic Properties of AMoO$_4$ (A = Ca, Ba) Particles Synthesized *via* Cyclic Microwave-Assisted Metathetic Route

Chang Sung Lim

Department of Advanced Materials Science & Engineering, Hanseo University, Seosan 356-706, Republic of Korea

Corresponding author: Tel/Fax: +82 41 6601445; E-mail: cslim@hanseo.ac.kr

AMoO$_4$ (A=Ca, Ba) particles have been successfully synthesized *via* cyclic microwave-assisted metathetic route in ethylene glycol followed by further heat-treatment. The AMoO$_4$ (A=Ca, Ba) particles were well crystallized after heat-treatment at 400-600 °C for 3 h. The microstructures exhibited fine morphologies with sizes of 0.5-1 and 1.5-2 µm for the CaMoO$_4$ and BaMoO$_4$ particles, respectively. The synthesized AMoO$_4$ (A=Ca, Ba) particles were characterized by X-ray diffraction, scanning electron microscopy. Other spectroscopic properties were also examined using photoluminescence emission measurements and Raman spectroscopy.

**Keywords: Microstructure, AMoO$_4$ (A=Ca, Ba), Microwave-assisted metathetic route, Photoluminescence, Raman spectroscopy.**

## INTRODUCTION

Metal molybdates have attracted considerable attention for potential applications in photoluminescence, hosts for lanthanide-activated lasers, photocatalysis and humidity sensors[1-3]. The physical, chemical and photochemical properties of metal molybdates are dependent on the manufacturing method. Several processes have been developed over the past decade to enhance the applications of metal molybdates, such as co-precipitation[4], the electrochemical technique[5], aqueous mineralization process[6], the hydrothermal method[7,8], the microwave-hydrothermal method[9,10], the microwave-assisted polymerized complex method[11,12], pulsed laser ablation[13] and the microwave assisted synthesis in solution[14]. Among different methods, solution-based chemical synthetic methods play the key role in the design and production of fine oxide powders and are successful in overcoming many limitations of traditional solid-state, high-temperature methods.

As compared to common methods, the microwave synthesis technique provides such advantages as a short reaction time, small particle size, narrow particle size distribution and it is the high purity method suitable for the preparation of poly-crystalline products. The microwave heating is delivered to the surface of the material by radiant and/or convection heating, which is transferred to the bulk of the material *via* conduction. So, the microwave energy is delivered directly to the material through the molecular interactions with electromagnetic field. Heat can be generated through volumetric heating because microwaves can penetrate the material and supply energy[15-18].

In this study, the AMoO$_4$ (A=Ca, Ba) particles were synthesized by a microwave-assisted metathetic method in ethylene glycol. The synthesized AMoO$_4$ (A=Ca, Ba) particles were characterized by X-ray diffraction (XRD), scanning electron microscopy (SEM). Their spectroscopic properties were examined by photoluminescence (PL) emission and Raman spectroscopy.

## EXPERIMENTAL

CaCl$_2$, BaCl$_2$·2H$_2$O and Na$_2$MoO$_4$·2H$_2$O of analytic reagent grade were used to prepare the AMoO$_4$ (A=Ca, Ba) particles by a cyclic microwave-assisted metathetic reaction in ethylene glycol. For the metathetic reaction of CaMoO$_4$, 0.01 mol each of CaCl$_2$ and Na$_2$WO$_4$·2H$_2$O were dissolved in 30 mL ethylene glycol, respectively. For the metathetic reaction of BaMoO$_4$, 0.01 mol each of BaCl$_2$·2H$_2$O and Na$_2$MoO$_4$·2H$_2$O were dissolved in 30 mL of ethylene glycol, respectively. After the complete homogeneous stirring of each solution, they were mixed together and stirred until the solution became more viscous and transparent. The solutions were mixed and adjusted to pH 9.5 using NaOH. The aqueous solutions were then stirred at room temperature. In the sequence, the mixtures were transferred into a Teflon vessel with a capacity of 120 mL. The Teflon vessel was heated in a microwave oven operating at a frequency of 2.45 GHz and a maximum output power of 1250 W for 23 min. The working cycle of the microwave-assisted metathetic reaction was controlled precisely and consisted of 30 s on and 30 s off for 10 min, followed by 30 s on and 60 s off for a further 20 min. The resulting samples were treated with ultrasonic radiation

and washed many times with hot distilled water. The white precipitates were collected and dried at 100 °C in a dry oven. The final products were heat-treated at 400-600 °C for 3 h.

The existing phase in the particles after the metathetic reactions and heat-treatment was identified by powder XRD (CuKα, Rigaku D/MAX 2200, Japan). The microstructure and surface morphology of the $AMoO_4$ (A=Ca, Ba) particles were observed by SEM (JSM-5600, JEOL, Japan). The photoluminescence spectra were recorded using a spectrophotometer (Perkin Elmer LS55, UK) at room temperature. Raman spectroscopy was performed using a LabRam HR (Jobin-Yvon, France). The 514.5 nm line of an Ar-ion laser was used as the excitation source and the power applied to the samples was kept at 0.5 mW.

## RESULTS AND DISCUSSION

Fig. 1 shows the XRD patterns of the (a) $CaMoO_4$ and (b) $BaMoO_4$ particles synthesized by the cyclic microwave-assisted metathetic reaction in ethylene glycol. All the XRD peaks were assigned to $CaMoO_4$ and $BaMoO_4$ with a Scheelite-type structure, which are in good agreement with the crystallographic data of $CaMoO_4$ (JCPDS: 85-0585) and $BaMoO_4$ (JCPDS: 29-01930), respectively. The crystallized $CaMoO_4$ and $BaMoO_4$ particles were prepared using a metathetic reaction in ethylene glycol assisted by cyclic microwave irradiation. These XRD peaks were the same as those of the $CaMoO_4$ and $BaMoO_4$ particles after heat-treatment at 400-600 °C for 3 h. The $CaMoO_4$ had a Scheelite-type crystal structure with lattice parameters of a = b = 5.212 Å and c = 11.438 Å[14], whereas

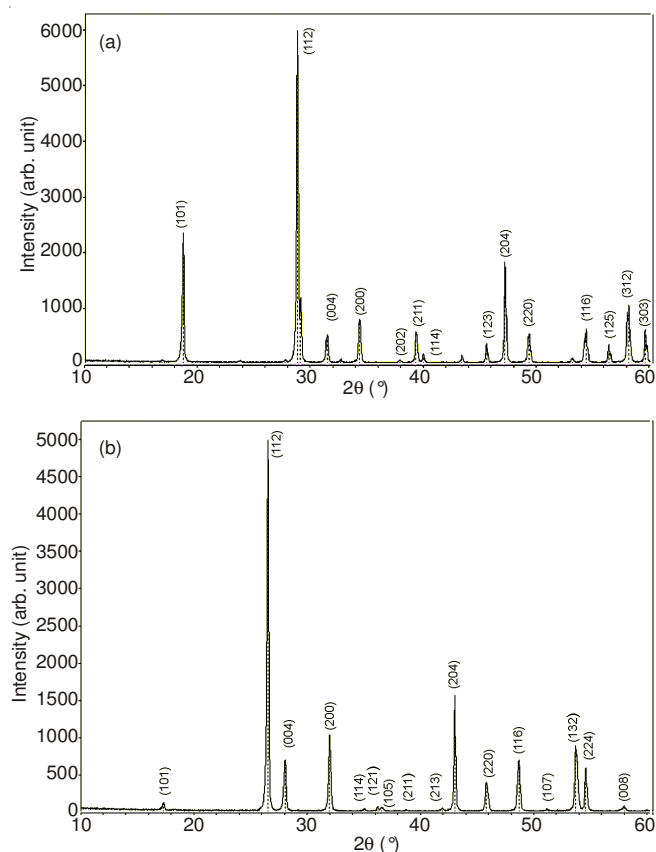the $BaMoO_4$ formed had Scheelite-type crystal structure with lattice parameters of a = b = 5.573 Å and c = 12.786 Å[18]. The metathetic reactions in ethylene glycol assisted by cyclic microwave irradiation are suitable for the growth of the $CaMoO_4$ and $BaMoO_4$ crystallites responsible for the strongest intensity peaks from the (112), (200) and (312) planes, which were the major peaks of the $CaMoO_4$ and $BaMoO_4$.

Fig. 2 shows the SEM images of the synthesized (a) $CaMoO_4$ and (b) $BaMoO_4$ particles after heat-treatment 600 °C for 3 h. The $AMoO_4$ (A=Ca, Ba) particles were well crystallized after heat-treatment at 600 °C for 3 h. The SEM image of the $CaMoO_4$ particles in Fig. 2a revealed fine morphology with a size of 0.5-1 μm. The SEM image of the $BaMoO_4$ particles in Fig. 2b exhibited well crystallized morphologies with a size of 1.5-2 μm. The microwave-assisted metathetic reaction provides the exothermic energy required to synthesize the metal molybdates. In addition, it enables the bulk of the material to be heated uniformly, resulting in fine particles with a controlled morphology and the product to be fabricated in a green manner without the generation of solvent waste. Metathetic reactions, such as $CaCl_2 + Na_2MoO_4 \rightarrow CaMoO_4 + 2NaCl$ and $BaCl_2 + Na_2MoO_4 \rightarrow BaMoO_4 + 2NaCl$, involve the exchange of atomic/ionic species, in which the driving force is the exothermic reaction accompanying the formation of $NaCl$[20]. The $CaMoO_4$ and $BaMoO_4$ particles were heated rapidly and uniformly by
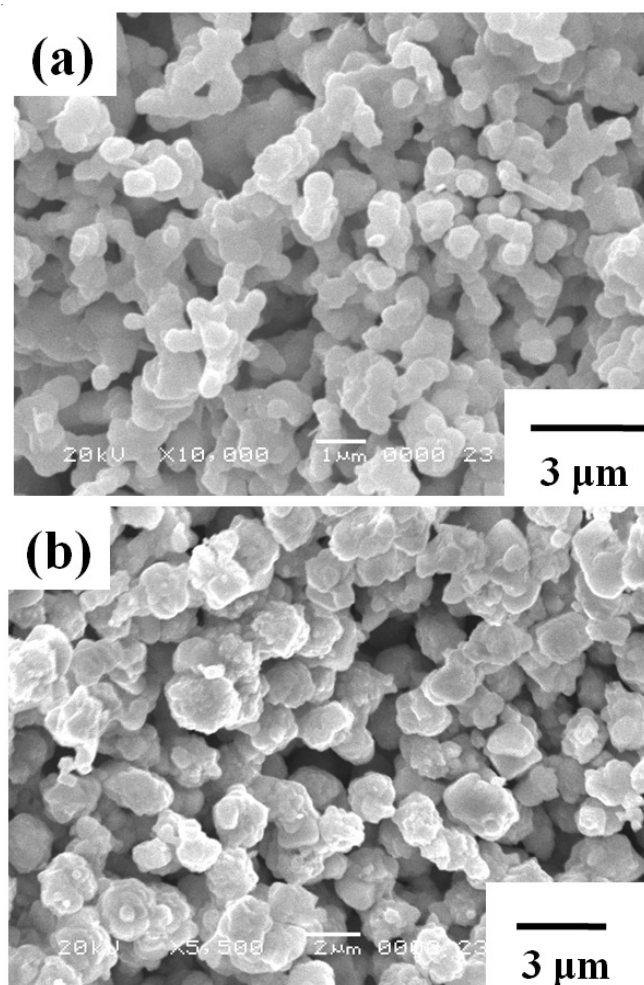


Fig. 2. SEM images of the synthesized (a) $CaMoO_4$ and (b) $BaMoO_4$ particles



Fig. 1. XRD patterns of the synthesized (a) $CaMoO_4$ and (b) $BaMoO_4$ particles

the cyclic microwave-assisted metathetic route. This classifies the method among simple and cost-effective ones and, evidently, the microwave-assisted metathetic technology is able to provide high yields with an easy scale-up as a viable alternative for the rapid synthesis of complex oxide composites[19]. The microwave-assisted metathetic reaction and post heat-treatment are interdependent and essential procedures to synthesize well defined $AMoO_4$ (A=Ca, Ba) particles. For the molybdate materials to be used for practical applications, it is necessary to control the size distribution and morphology of the particles.

Fig. 3 presents the photoluminescence emission spectra of the $CaMoO_4$ particles after heat-treatment at (a) 400 °C for 3 h, (b) 500 °C for 3 h and (c) 600 °C for 3 h excited at 250 nm at room temperature. With excitation at 250 nm, the $CaMoO_4$ particles exhibit a photoluminescence emission in the green wavelength range of 480-500 nm. The intensity increases with increasing heat-treatment temperature. The photoluminescence intensity of phosphors strongly depends on the particle shape and distribution. Generally, for similar morphological samples, homogenized particles have better luminescent characteristics, because of the lesser contamination or fewer dead layers on the phosphor surface. The strong photoluminescence intensity was attributed to their well-defined and homogeneous morphology with sizes of 0.5-1 μm.
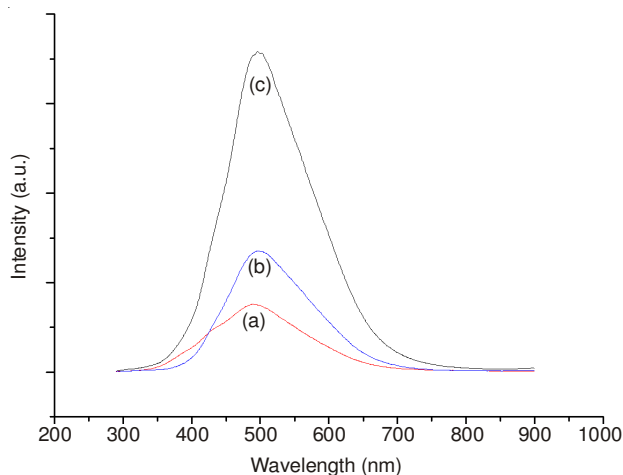
Fig. 3.  Photoluminescence emission spectra of the $CaMoO_4$ particles after heat-treatment at (a) 400 °C for 3 h, (b) 500 °C for 3 h and (c) 600 C for 3 h excited at 250 nm at room temperature

Fig. 4 shows the photoluminescence emission spectra of the $BaMoO_4$ particles after heat-treatment at (a) 400 °C for 3 h, (b) 500 °C for 3 h and (c) 600 °C for 3 h excited by 250 nm at room temperature. The emission spectrum of metal molybdates is due mainly to charge-transfer transitions within the $[MoO_4]^{2-}$ complex[20,21]. With excitation at 250 nm, the $BaMoO_4$ particles exhibit a photoluminescence emission in the blue wavelength range of 370-420 nm. The photoluminescence spectra of the $CaMoO_4$ and $BaMoO_4$ particles after heat-treatment at 400-600 °C for 3 h shown in Figs. 4 and 5, respectively, show the same peak positions. The photoluminescence intensities of the $CaMoO_4$ and $BaMoO_4$ particles prepared at 600 °C are stronger than those of the samples prepared at 400 and 500 °C. This suggests that the photoluminescence intensity depends on the crystallinity of the $CaMoO_4$ and $BaMoO_4$ particles. Their high

crystallinity plays an important role in improving the luminescent efficiency. Therefore, the enhancement of the photoluminescence intensity with increasing heat-treatment temperature up to 600 °C is due to the increase in crystallinity. The photoluminescence intensity of energy-conversion materials depends strongly on the particle shape and distribution. Generally, for similar morphological samples, homogenized particles are favorable to the luminescent characteristics, because of the lesser contamination or fewer dead layers on the surface of the energy-conversion materials.
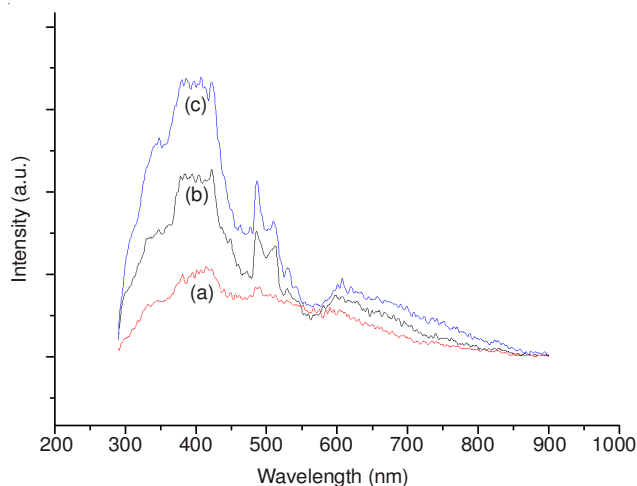
Fig. 4.  Photoluminescence emission spectra of the $BaMoO_4$ particles after heat-treatment at (a) 400 °C for 3 h, (b) 500 °C for 3 h and (c) 600 °C for 3 h excited at 250 nm at room temperature
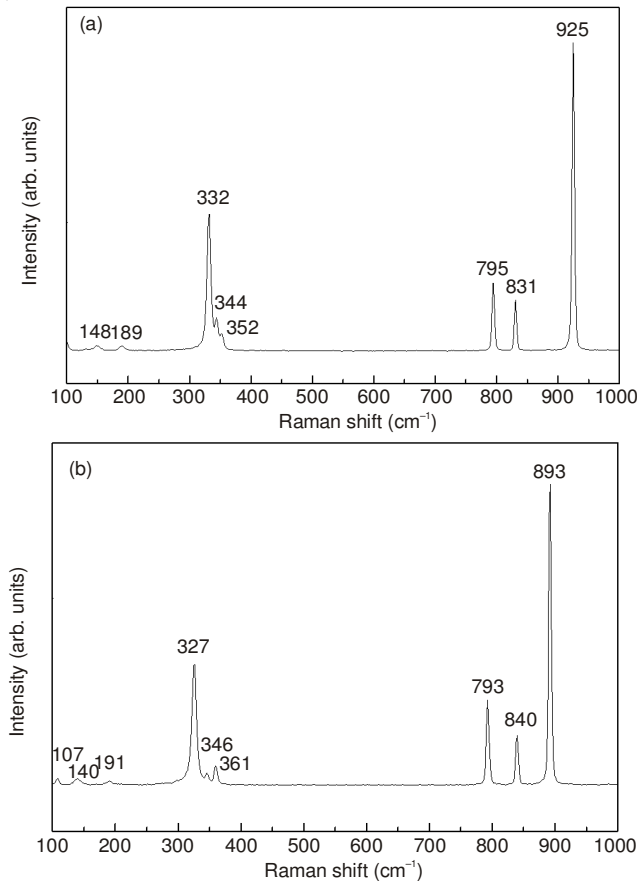
Fig. 5.  Raman spectra of the synthesized (a) $CaMoO_4$ and (b) $BaMoO_4$ particles

The four narrow shoulders in the emission spectra at approximately 480, 500, 520 and 600 nm are believed to be due to a defect structure[22]. Such peaks, namely the "spread-eagle" shape of the blue emission, can be explained by the influence of the Jahn-Teller effect[23,24] on the degenerated excited state of the $[MoO_4]^{2-}$ tetrahedron. Generally, the presence of Gaussian components indicates that the electronic levels corresponding to the relaxed excited state of an emission centre belong to a degenerate excited state influenced by some perturbation, *e.g.* a local low symmetry crystal field[22]. The Jahn-Teller splitting effect essentially determines the emission shape of the $AMoO_4$ (A= Ca, Ba) particles. The additional emission bands can be explained by the existence of a Frenkel defect structure (oxygen ion shifted to the inter-position with the simultaneous creation of vacancies) in the surface layers of the $BaMoO_4$ particles[25].

Fig. 5 shows the Raman spectra of the (a) $CaMoO_4$ and (b) $BaMoO_4$ particles after heat-treatment at 600 °C for 3 h excited by the 514.5 nm line of an Ar-ion laser at 0.5 mW. The vibration modes in the Raman spectra of molybdates can be classified into two groups, *viz.* internal and external[26,27]. The internal modes for the $CaMoO_4$ particles in Fig. 5a were detected as the $\nu_1(A_g)$, $\nu_3(B_g)$, $\nu_3(E_g)$, $\nu_4(E_g)$, $\nu_4(B_g)$ and $\nu_2(B_g)$ vibrations at 925, 831, 795, 352, 344 and 332 cm$^{-1}$, respectively. The free rotation mode was detected at 189 cm$^{-1}$ and the external mode was localized at 148 cm$^{-1}$. The internal modes of the $BaMoO_4$ particles in Fig. 5b were detected as the $\nu_1(A_g)$, $\nu_3(B_g)$, $\nu_3(E_g)$, $\nu_4(E_g)$, $\nu_4(B_g)$ and $\nu_2(B_g)$ vibrations at 893, 840, 793, 361, 346 and 327 cm$^{-1}$, respectively. The free rotation mode was detected at 191 and 140 cm$^{-1}$ and the external modes were localized at 107 cm$^{-1}$. The well-resolved sharp peaks for the synthesized $CaMoO_4$ and $BaMoO_4$ particles indicate that they are highly crystallized.

**Conclusion**

$AMoO_4$ (A=Ca, Ba) particles were successfully synthesized *via* microwave-assisted metathetic route in ethylene glycol followed by further heat treatment. After heat-treatment at 600 °C for 3 h, the $CaMoO_4$ particles exhibited fine morphologies with sizes of 0.5-1 μm, whereas the $BaMoO_4$ particles exhibited well crystallized morphologies with sizes of 1.5-2 μm. With excitation at 250 nm, the $CaMoO_4$ particles exhibited strong photoluminescence emissions in the green wavelength range of 480-500 nm, whereas the $BaMoO_4$ particles exhibited photoluminescence emissions in the blue wavelength range of 370-420 nm. The photoluminescence intensities of the $CaMoO_4$ and $BaMoO_4$ particles prepared at 600 °C are stronger than those of the samples prepared at 400 and 500 °C. The well-resolved internal mode peaks in the Raman spectra for the $CaMoO_4$ particles at 925, 831, 795, 352, 344 and 332 cm$^{-1}$ were observed in addition to the free rotation mode at 189 cm$^{-1}$ and the external mode at 148 cm$^{-1}$, whereas those in the spectra of the $BaMoO_4$ particles were observed at 893, 840, 793, 361,

346 and 327 cm$^{-1}$ in addition to the free rotation mode at 191 and 140 cm$^{-1}$ and the external modes at 107 cm$^{-1}$, indicating highly crystalline particles.

## REFERENCES

1.  S. Rajagopal, V.L. Bekenev, D. Nataraj, D. Mangalaraj and O.Y. Khyzhun, *J. Alloys Compd.*, **496**, 61 (2010).
2.  L. Zhen, W.S. Wang, C.Y. Xu, W.Z. Shao, M.M. Ye and Z.L. Chen, *Scr. Mater.*, **58**, 461 (2008).
3.  R.N. Singh, J.P. Singh and A. Singh, *Int. J. Hydrogen Energy*, **33**, 4260 (2008).
4.  X. Zhao, T.L.Y. Cheung, Y. Xi, K.C. Chung, D.H.L. Ng and J. Yu, *J. Mater. Sci.*, **42**, 6716 (2007).
5.  P. Yu, J. Bi, D.J. Gao, Q. Xiao, L.P. Chen, X.L. Jin and Z.N. Yang, *J. Electroceram.*, **21**, 184 (2008).
6.  X. Wu, J. Du, H. Li, M. Zhang, B. Xi, H. Fan, Y. Zhu and Y. Qian, *J. Solid State Chem.*, **180**, 3288 (2007).
7.  G. Zhang, S. Yu, Y. Yang, W. Jiang, S. Zhang and B. Huang, *J. Cryst. Growth*, **312**, 1866 (2010).
8.  K. Eda, Y. Kato, Y. Ohshiro, T. Sugitani and M.S. Whittingham, *J. Sol. State Chem.*, **183**, 1334 (2010).
9.  J.T. Kloprogge, M.L. Weier, L.V. Duong and R.L. Frost, *Mat. Chem. Phys.*, **88**, 438 (2004).
10. L.S. Cavalcante, J.C. Sczancoski, R.L. Tranquilin, J.A. Varela, E. Longo and M.O. Orlandi, *Particuology*, **7**, 353 (2009).
11. J.H. Ryu, J.W. Yoon, C.S. Lim, W.C. Oh and K.B. Shim, *J. Alloys Comp.*, **390**, 245 (2005).
12. J.H. Ryu, B.G. Choi, S.H. Kim, J.W. Yoon, C.S. Lim and K.B. Shim, *Mater. Res. Bull.*, **40**, 1468 (2005).
13. J.H. Ryu, B.G. Choi, J.-W. Yoon, K.B. Shim, K. Machi and K. Hamada, *J. Lumin.*, **124**, 67 (2007).
14. T. Thongtem, A. Phuruangrat and S. Thongtem, *Mater. Lett.*, **62**, 454 (2008).
15. T. Trongtem, A. Phuruangrat and S. Trongtem, *J. Nanopart. Res.*, **12**, 2287 (2010).
16. C.S. Lim, *Mater. Res. Bull.*, **47**, 4220 (2012).
17. C.S. Lim, *Asian J. Chem.*, **25**, 63 (2013).
18. S. Das, A.K. Mukhopadhyay, S. Datta and D. Basu, *Bull. Mater. Sci.*, **32**, 1 (2009).
19. C.S. Lim, *Mater. Chem. Phys.*, **131**, 714 (2012).
20. D.A. Spassky, S.N. Ivanov, V.N. Kolobanov, V.V. Mikhailin, V.N. Zemskov, B.I. Zadneprovski and L.I. Potkin, *Radiat. Meas.*, **38**, 607 (2004).
21. G.Y. Hong, B.S. Jeon, Y.K. Yoo and J.S. Yoo, *J. Electrochem. Soc.*, **148**, H161 (2001).
22. K. Polak, M. Nikl, K. Nitsch, M. Kobayashi, M. Ishii, Y. Usuki and O. Jarolimek, *J. Lumin.*, **72-74**, 781 (1997).
23. Y. Toyozawa and M. Inoue, *J. Phys. Soc. Jpn.*, **21**, 1663 (1966).
24. E.G. Reut, *Izv. Akad. Nauk SSSR, Ser. Fiz.*, **43**, 1186 (1979).
25. V.B. Mikhailik, H. Kraus, D. Wahl and M.S. Mykhaylyk, *Phys. Status Solid B*, **242**, R17 (2005).
26. T.T. Basiev, A.A. Sobol, Y.K. Voronko and P.G. Zverev, *Opt. Mat.*, 15, 205 (2000).
27. T.T. Basiev, A.A. Sobol, P.G. Zverev, L.I. Ivleva, V.V. Osiko and R.C. Powell, *Opt. Mater.*, **11**, 307 (1999).